PROCEEDINGS OF SCIENCE

Axial couplings of heavy hadrons from domain-wall lattice QCD

William Detmold[a,b], **C.-J. David Lin**[c,d], **Stefan Meinel**[*a]

[a] *Department of Physics, College of William & Mary, Williamsburg, VA 23187-8795, USA*
[b] *Jefferson Laboratory, 12000 Jefferson Avenue, Newport News, VA 23606, USA*
[c] *Institute of Physics, National Chiao-Tung University, Hsinchu 300, Taiwan*
[d] *Physics Division, National Centre for Theoretical Sciences, Hsinchu 300, Taiwan*

E-mail: smeinel@wm.edu

We calculate matrix elements of the axial current for static-light mesons and baryons in lattice QCD with dynamical domain wall fermions. We use partially quenched heavy hadron chiral perturbation theory in a finite volume to extract the axial couplings g_1, g_2, and g_3 from the data. These axial couplings allow the prediction of strong decay rates and enter chiral extrapolations of most lattice results in the b sector. Our calculations are performed with two lattice spacings and with pion masses down to 227 MeV.

The XXIX International Symposium on Lattice Field Theory - Lattice 2011
July 10-16, 2011
Squaw Valley, Lake Tahoe, California

[*]Speaker.

PoS(Lattice 2011)166

1. Introduction

The low-energy dynamics of heavy-light mesons and baryons can be described by heavy-hadron chiral perturbation theory (HHχPT), an effective field theory for QCD that incorporates both chiral symmetry and heavy-quark symmetry [1]. HHχPT is essential for controlling light-quark-mass extrapolations of lattice QCD data in the heavy-quark sector (see for example Ref. [2]).

At leading order in the heavy-quark and chiral expansions, the HHχPT Lagrangian contains three axial coupling constants that determine the strength of the interactions between heavy-light hadrons and pions: one coupling (denoted as g_1) for the heavy-light mesons, and two additional couplings (denoted as g_2, g_3) for the heavy-light baryons. These axial couplings are calculable from QCD, and their determination enables quantitative predictions for many heavy-light hadron properties (such as masses, decay widths, and various matrix elements) using HHχPT. The chiral loop contributions that lead to the nonanalytic dependence of such properties on the light-quark masses are proportional to products of the relevant axial couplings. While g_1 has received much attention in the past because of its role for B mesons, the lesser-known couplings g_2 and g_3 are important for flavor physics with heavy baryons. The bottom baryon sector provides complementary information to B mesons for constraining the helicity structure of possible new physics [3].

The calculation of $g_{1,2,3}$ from the underlying theory of QCD must be done nonperturbatively, and hence on a lattice. The mesonic coupling g_1 had been studied previously in lattice QCD with $n_f = 0$ or $n_f = 2$ dynamical flavors [4]. In the following, we present a complete determination of all three axial couplings $g_{1,2,3}$ using $n_f = 2+1$ domain-wall lattice QCD [5, 6]. Our choice of lattice parameters (low pion masses, large volume, two lattice spacings) and our analysis method (fits to the axial-current matrix elements using the correct next-to-leading-order formulae from HHχPT [7]) allow us to control all sources of systematic uncertainties.

2. Heavy-hadron chiral perturbation theory

We begin with an introduction to HHχPT. This theory combines the chiral expansion with an expansion in powers of Λ_{QCD}/m_Q, where m_Q is the heavy-quark mass. We work at the leading order in the heavy-quark expansion, where the spin of the light degrees of freedom (s_l) is conserved and the heavy-quark spin decouples. The lowest-lying heavy-light mesons with $s_l = 1/2$ form multiplets with $J = 0$ and $J = 1$, which can be combined into a single field H^i:

$$H^i = \left[-P^i\gamma_5 + P^{*i}_\mu\gamma^\mu\right]\frac{1-\slashed{v}}{2}, \quad \text{with} \quad (P^i) = \begin{pmatrix} B^+ \\ B^0 \end{pmatrix}, \quad (P^{*i})_\mu = \begin{pmatrix} B^{*+} \\ B^{*0} \end{pmatrix}_\mu. \tag{2.1}$$

(We consider $SU(2)$ HHχPT and use the notation for bottom hadrons.) Similarly, the baryons with $s_l = 1$ form multiplets with $J = 1/2$ and $J = 3/2$. These are described by Dirac and Rarita-Schwinger fields B^{ij} and B^{*ij}_μ, which are symmetric in the flavor indices and can be combined into a single field S^{ij}:

$$S^{ij}_\mu = \sqrt{\frac{1}{3}}(\gamma_\mu + v_\mu)\gamma_5 B^{ij} + B^{*ij}_\mu, \quad \text{with} \quad (B^{ij}) = \begin{pmatrix} \Sigma_b^+ & \frac{1}{\sqrt{2}}\Sigma_b^0 \\ \frac{1}{\sqrt{2}}\Sigma_b^0 & \Sigma_b^- \end{pmatrix}, \quad (B^{*ij})_\mu = \begin{pmatrix} \Sigma_b^{*+} & \frac{1}{\sqrt{2}}\Sigma_b^{*0} \\ \frac{1}{\sqrt{2}}\Sigma_b^{*0} & \Sigma_b^{*-} \end{pmatrix}_\mu. \tag{2.2}$$

On the other hand, the $s_l = 0$ baryons ($J = 1/2$) are antisymmetric in flavor and include only the Λ_b in the $SU(2)$ case:

$$(T^{ij}) = \frac{1}{\sqrt{2}} \begin{pmatrix} 0 & \Lambda_b \\ -\Lambda_b & 0 \end{pmatrix}. \tag{2.3}$$

The leading-order HHχPT Lagrangian, describing the interactions of the fields (2.1), (2.2), and (2.3) with pions, is given by

$$\begin{aligned} \mathscr{L} \;=\; &(\text{ kinetic terms }) + g_1 \,\mathrm{tr_D}\left[\overline{H}_i(\mathscr{A}^\mu)^i{}_j\gamma_\mu\gamma_5 H^j\right] \\ &- i\,g_2\,\varepsilon_{\mu\nu\sigma\lambda}\overline{S}^\mu_{ki}v^\nu(\mathscr{A}^\sigma)^i{}_j(S^\lambda)^{jk} + \sqrt{2}\,g_3\left[\overline{S}^\mu_{ki}(\mathscr{A}_\mu)^i{}_jT^{jk} + \overline{T}_{ki}(\mathscr{A}^\mu)^i{}_jS^{jk}_\mu\right]. \end{aligned} \tag{2.4}$$

In the terms with g_1, g_2, and g_3, the pion field $\xi = \sqrt{\Sigma} = \exp(i\Phi/f)$ appears through

$$\mathscr{A}^\mu = \frac{i}{2}\left(\xi^\dagger\partial^\mu\xi - \xi\partial^\mu\xi^\dagger\right) = -\frac{1}{f}\partial^\mu\Phi + \ldots, \tag{2.5}$$

which is an axial-vector field.

3. Axial current matrix elements

To determine the axial couplings g_i that appear in the chiral Lagrangian (2.4) from QCD, one can calculate suitable hadronic observables in both HHχPT and lattice QCD. The expressions derived from HHχPT are then fitted to the lattice data, and in these fits the axial couplings are parameters. The simplest observables that are sensitive to g_i are the zero-momentum matrix elements of the axial current between heavy-hadron states. In QCD, the isovector axial current is given by the quark current

$$A^{a(\mathrm{QCD})}_\mu = \bar{q}\frac{\tau^a}{2}\gamma_\mu\gamma_5 q. \tag{3.1}$$

The corresponding hadronic current in HHχPT can be obtained from the Lagrangian (2.4) using the Noether procedure. At leading order, the relevant part of the current that contributes to the matrix elements reads

$$\begin{aligned} A^{a(\chi\mathrm{PT,LO})}_\mu \;=\; &g_1\,\mathrm{tr_D}\left[\overline{H}_i(\tau^a_{\xi+})^i{}_j\gamma_\mu\gamma_5H^j\right] - ig_2\,\varepsilon^{\mu\nu\sigma\lambda}(\overline{S}_\nu)_{ki}v_\sigma(\tau^a_{\xi+})^i{}_jS^{jk}_\lambda \\ &+\sqrt{2}\,g_3\left[(\overline{S}_\mu)_{ki}(\tau^a_{\xi+})^i{}_jT^{jk} + \overline{T}_{ki}(\tau^a_{\xi+})^i{}_j(S_\mu)^{jk}\right], \end{aligned} \tag{3.2}$$

with $\tau^a_{\xi+} = \frac{1}{2}\left(\xi^\dagger\tau^a\xi + \xi\tau^a\xi^\dagger\right)$. One finds the following matrix elements for $A_\mu = A^1_\mu - iA^2_\mu$,

$$\begin{aligned} \langle P^{*d}|A_\mu|P^u\rangle &= -2\,(g_1)_{\mathrm{eff}}\;\varepsilon^*_\mu, \\ \langle S^{dd}|A_\mu|S^{du}\rangle &= -(i/\sqrt{2})\,(g_2)_{\mathrm{eff}}\;v^\sigma\,\varepsilon_{\sigma\mu\nu\rho}\,\overline{U}^\nu U^\rho, \\ \langle S^{dd}|A_\mu|T^{du}\rangle &= -(g_3)_{\mathrm{eff}}\;\overline{U}_\mu\,\mathscr{U}, \end{aligned} \tag{3.3}$$

where ε^μ is the polarization vector of the P^{*d} meson and $\mathscr{U}$ is the Dirac spinor of the T^{du} baryon. For the $s_l = 1$ baryons, we work directly with external S^{ij} states (which contain the degrees of freedom of both $J = 1/2$ and $J = 3/2$) and the U^μ's are the corresponding generalized spinors [6]. At leading order in the chiral expansion, the "effective axial couplings" in (3.3) are equal to the

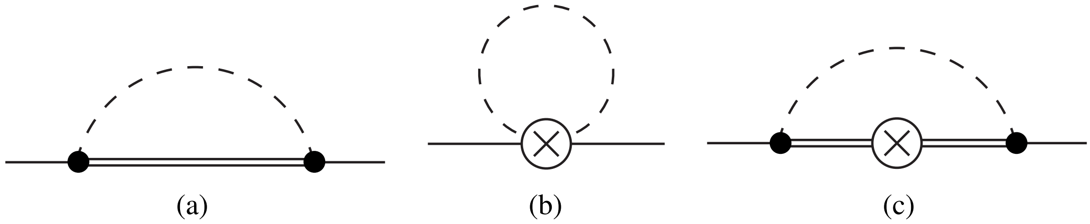

Figure 1: One-loop diagrams contributing to the matrix elements of the axial current in HHχPT: (a) wavefunction renormalization diagram, (b) tadpole diagram, (c) sunset diagram [7].

axial couplings in the Lagrangian, $(g_i)_{\rm eff}\big|_{\rm LO} = g_i$. At next-to-leading order, the matrix elements receive corrections from pion loops (Fig. 1) and analytic counterterms. The NLO expressions for $(g_i)_{\rm eff}$, both in the unquenched and the partially quenched theories, and for a finite volume, can be found in Ref. [7].

4. Lattice calculation

To calculate the matrix elements (3.3) in lattice QCD, we use the following interpolating fields for the heavy hadrons,

$$\begin{aligned} P^i &= (\gamma_5)_{\alpha\beta}\, \overline{Q}_{a\alpha}\, \tilde{q}^i_{a\beta}, & P^{*i}_\mu &= (\gamma_\mu)_{\alpha\beta}\, \overline{Q}_{a\alpha}\, \tilde{q}^i_{a\beta}, \\ S^{ij}_{\mu\,\alpha} &= \epsilon_{abc}\, (C\gamma_\mu)_{\beta\gamma}\, \tilde{q}^i_{a\beta}\, \tilde{q}^j_{b\gamma}\, Q_{c\alpha}, & T^{ij}_\alpha &= \epsilon_{abc}\, (C\gamma_5)_{\beta\gamma}\, \tilde{q}^i_{a\beta}\, \tilde{q}^j_{b\gamma}\, Q_{c\alpha}, \end{aligned} \tag{4.1}$$

where $\tilde{q}^i$ denotes a smeared light-quark field of flavor i, and Q denotes the static heavy quark field (here we set $v = (1,0,0,0)$). Just as in HHχPT, the interpolating field $S^{ij}_{\mu\,\alpha}$ couples to both the $J = 1/2$ and $J = 3/2$ baryon states with $s_l = 1$. We use the domain-wall action [8] for the light quarks, and the Eichten-Hill action [9] with HYP-smeared temporal gauge links [10] for the heavy quarks. To optimize the signals and analyze heavy-quark discretization effects, we generated data for $n_{\rm HYP} = 1,2,3,5,10$ levels of HYP smearing. The final results for the axial couplings are based on data with $n_{\rm HYP} = 1,2,3$ only. The calculations are performed with the local 4-dimensional axial current, given by

$$A_\mu = Z_A\, \overline{d}_{a\alpha} (\gamma_\mu \gamma_5)_{\alpha\beta}\, u_{a\beta}, \tag{4.2}$$

where Z_A is determined nonperturbatively [11]. We compute the following ratios of three-point and two-point functions,

$$\begin{aligned} R_1(t,\,t') &= -\frac{1}{3}\frac{\sum_{\mu=1}^3 \langle\, P^{*d\,\mu}(t)\, A^\mu(t')\, P^\dagger_u(0)\,\rangle}{\langle\, P^u(t)\, P^\dagger_u(0)\,\rangle}, \\ R_2(t,\,t') &= i\, \frac{\sum_{\mu,\nu,\rho=1}^3 \varepsilon_{0\mu\nu\rho}\, \langle\, S^{dd\,\mu}(t)\, A^\nu(t')\, \overline{S}^\rho_{du}(0)\,\rangle}{\sum_{\mu=1}^3 \langle\, S^{dd\,\mu}(t)\, \overline{S}^\mu_{dd}(0)\,\rangle}, \\ R_3(t,\,t') &= \left[\frac{1}{3}\frac{\sum_{\mu,\nu=1}^3 \langle\, S^{dd\,\mu}(t)\, A^\mu(t')\, \overline{T}_{du}(0)\,\rangle \langle\, T^{du}(t)\, A^{\nu\dagger}(t')\, \overline{S}^\nu_{dd}(0)\,\rangle}{\sum_{\mu=1}^3 \langle\, S^{dd\,\mu}(t)\, \overline{S}^\mu_{dd}(0)\,\rangle \langle\, T^{du}(t)\, \overline{T}_{du}(0)\,\rangle}\right]^{1/2}, \end{aligned} \tag{4.3}$$

where the source and sink hadron interpolating fields are placed at a common spatial point $\mathbf{x}$ because of the static heavy quark, and we write $A^\mu(t') = \sum_{\mathbf{x}'} A^\mu(t',\mathbf{x}')$. In Eq. (4.3) we also removed

$L^3 \times T$	$am_{u/d}^{(\mathrm{sea})}$	$am_{u/d}^{(\mathrm{val})}$	a (fm)	$m_\pi^{(\mathrm{vv})}$ (MeV)	$m_\pi^{(\mathrm{vs})}$ (MeV)	values of t/a
$24^3 \times 64$	0.005	0.005	0.1119(17)	336(5)	336(5)	4, 5, 6, 7, 8, 9, 10
$24^3 \times 64$	0.005	0.002	0.1119(17)	270(4)	304(5)	4, 5, 6, 7, 8, 9, 10
$24^3 \times 64$	0.005	0.001	0.1119(17)	245(4)	294(5)	4, 5, 6, 7, 8, 9, 10
$32^3 \times 64$	0.006	0.006	0.0848(17)	352(7)	352(7)	13
$32^3 \times 64$	0.004	0.004	0.0849(12)	295(4)	295(4)	6, 9, 12
$32^3 \times 64$	0.004	0.002	0.0849(12)	227(3)	263(4)	6, 9, 12

Table 1: Lattice parameters. $m_\pi^{(\mathrm{vv})}$ and $m_\pi^{(\mathrm{vs})}$ denote the valence-valence and valence-sea pion masses.

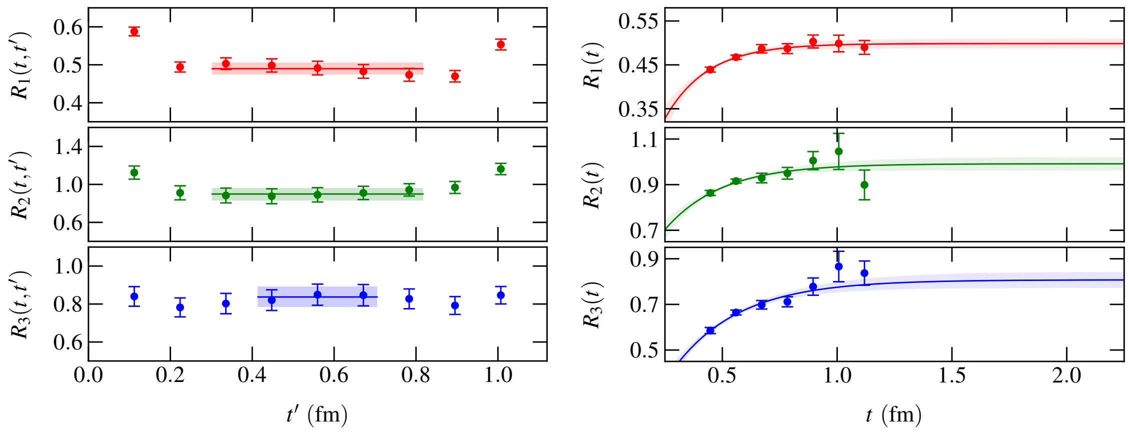

Figure 2: Left panel: ratios $R_i(t,t')$ for the source-sink separation $t/a = 10$, along with extracted values $R_i(t)$ (shaded regions). Right panel: extrapolation of $R_i(t)$ to infinite source-sink separation. All data shown here are for $a = 0.112$ fm, $am_{u,d}^{(\mathrm{val})} = 0.002$, $n_{\mathrm{HYP}} = 3$.

the free spinor indices which trivially originate from the static heavy-quark propagator. By inserting complete sets of states into (4.3), one can show that $R_i(t, t/2) = (g_i)_{\mathrm{eff}} + \ldots$, where the dots indicate contributions from excited states that decay exponentially with t [6].

Our calculations use RBC/UKQCD gauge field configurations with 2+1 dynamical quark flavors [11]. The main parameters of the ensembles and the domain-wall propagators we computed on them are given in Table 1. For the three-point functions we use pairs of light-quark propagators with sources at a common spatial point $\mathbf{x}$ and separated by t/a steps in the time direction. As can be seen in the table, we have data for multiple values of t/a. Numerical examples for the ratios (4.3) are shown in Fig. 2 (left). Equivalently to using $R_i(t, t/2)$, we average $R_i(t,t')$ over t' in the central plateau regions, and we denote these averages as $R_i(t)$. We then perform fits of the form $R_i(t) = (g_i)_{\mathrm{eff}} - A_i\, e^{-\delta_i t}$, as shown in Fig. 2 (right). A detailed discussion can be found in Ref. [6]. These fits provide the effective axial couplings $(g_i)_{\mathrm{eff}}(a, m_\pi^{(\mathrm{vv})}, m_\pi^{(\mathrm{vs})}, n_{\mathrm{HYP}})$ for all combinations of the lattice spacing, the pion masses, and the heavy-quark smearing parameter n_{HYP}. We fit the data for $(g_i)_{\mathrm{eff}}(a, m_\pi^{(\mathrm{vv})}, m_\pi^{(\mathrm{vs})}, n_{\mathrm{HYP}})$ with

$$\begin{aligned} (g_1)_{\mathrm{eff}} &= g_1\left[1 + f_1(g_1,\, m_\pi^{(\mathrm{vv})},\, m_\pi^{(\mathrm{vs})},\, L) + c_1^{(\mathrm{vv})}\,[m_\pi^{(\mathrm{vv})}]^2 + c_1^{(\mathrm{vs})}\,[m_\pi^{(\mathrm{vs})}]^2 + d_{1,n_{\mathrm{HYP}}}\, a^2\right], \\ (g_i)_{\mathrm{eff}}\Big|_{i=2,3} &= g_i\left[1 + f_i(g_2,\, g_3,\, m_\pi^{(\mathrm{vv})},\, m_\pi^{(\mathrm{vs})},\, \Delta,\, L) + c_i^{(\mathrm{vv})}\,[m_\pi^{(\mathrm{vv})}]^2 + c_i^{(\mathrm{vs})}\,[m_\pi^{(\mathrm{vs})}]^2 + d_{i,n_{\mathrm{HYP}}}\, a^2\right], \end{aligned} \tag{4.4}$$

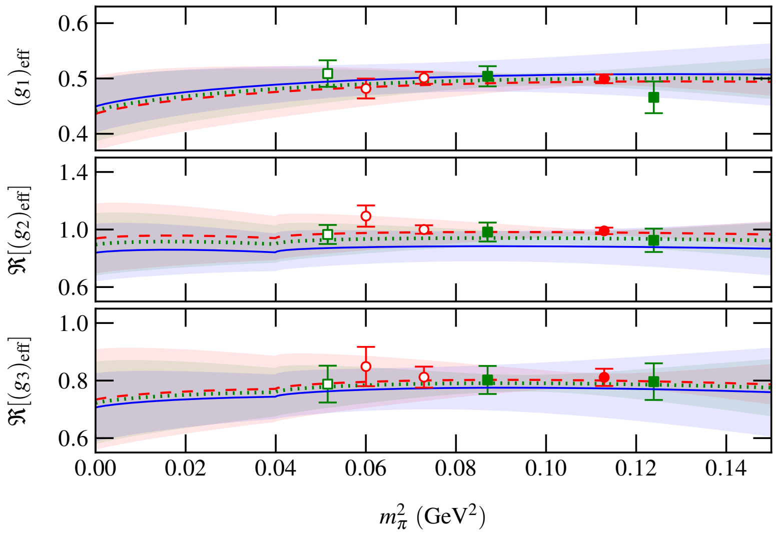

Figure 3: Fits of $(g_i)_{\rm eff}$ using Eq. (4.4). The plot shows the fitted functions, evaluated at $m_\pi^{(\rm vv)} = m_\pi^{(\rm vs)} = m_\pi$ and in infinite volume, for $n_{\rm HYP} = 3$. The baryonic matrix elements $(g_{2,3})_{\rm eff}$ develop small imaginary parts below the $S \to T\pi$ decay threshold at $m_\pi = \Delta$, and only the real parts are shown here. The dashed line corresponds to $a = 0.112$ fm, the dotted line to $a = 0.085$ fm, and the solid line to the continuum limit. The $\pm 1\sigma$ regions are shaded. The data points (circles: $a = 0.112$ fm, squares: $a = 0.085$ fm) have been shifted to infinite volume for this plot, and the partially quenched data ($m_\pi^{(\rm vv)} < m_\pi^{(\rm vs)}$) are included using open symbols at $m_\pi = m_\pi^{(\rm vv)}$, even though the fit functions have slightly different values for these points.

where the functions f_i are the NLO loop contributions from $SU(4|2)$ HHχPT, including the effects of the finite lattice size [5]. The terms with coefficients $c_i^{(\rm vv)}$ and $c_i^{(\rm vs)}$ are analytic NLO counterterms that cancel the renormalization-scale-dependence of f_i, and the terms with coefficients $d_{i,n_{\rm HYP}}$ describe the leading effects of the non-zero lattice spacing. The functions $f_{2,3}$ also depend on the $S-T$ mass splitting Δ, which is included in the kinetic terms of Eq. (2.4). We set $\Delta = 200$ MeV, consistent with the $\Sigma_b^{(*)} - \Lambda_b$ splitting from experiment and with our lattice data.

To study the effect of the HYP smearing in the heavy-quark action on the scaling behavior, we performed initial fits that included all values of $n_{\rm HYP}$, and then successively removed the data with the largest values of $n_{\rm HYP}$. After excluding $n_{\rm HYP} = 5, 10$, the fits were stable and had good Q-values. Our final results for the axial couplings are

$$\begin{aligned} g_1 &= 0.449 \pm 0.047_{\rm stat} \pm 0.019_{\rm syst}, \\ g_2 &= 0.84 \pm 0.20_{\rm stat} \pm 0.04_{\rm syst}, \\ g_3 &= 0.71 \pm 0.12_{\rm stat} \pm 0.04_{\rm syst}. \end{aligned} \tag{4.5}$$

The estimates of the systematic uncertainties in (4.5) include the effects of the following: NNLO terms in the fits to the a- and m_π-dependence (3.6%, 2.8%, 3.7% for g_1, g_2, g_3, respectively), the above-physical value of the sea-strange-quark mass (1.5%), and higher excited states in $R_i(t)$ (1.7%, 2.8%, 4.9%). The details of the analysis can be found in Ref. [6].

Figure 3 shows the pion-mass dependence of the fitted functions $(g_i)_{\rm eff}$. The counterterm parameters $c_i^{(\rm vv)}$ and $c_i^{(\rm vs)}$ resulting from the fits are natural-sized (for $\mu = 4\pi f_\pi$), and the NLO contributions are significantly smaller than the LO contributions. We conclude that the $SU(4|2)$ chiral expansion of $(g_i)_{\rm eff}$ convergences well for the pion masses used here.

5. Summary

We have calculated the heavy-hadron axial couplings using lattice QCD, including for the first time the baryonic couplings g_2 and g_3 in addition to the mesonic coupling g_1. The analysis is based on data for the axial-current matrix elements at low pion masses, a large volume, and two different lattice spacings. We extracted $g_{1,2,3}$ from this data by performing chiral fits with the full NLO expressions from HHχPT [7]. As a consequence, the systematic uncertainties in our results (4.5) are much smaller than the statistical uncertainties. The numerical values of $g_{1,2,3}$ can be used to constrain chiral fits of lattice QCD data for a wide range of heavy-light meson and baryon observables. Furthermore, our results for the axial couplings allow the direct calculation of certain observables in HHχPT, in particular the strong decay widths of heavy baryons [5, 6].

Acknowledgments: WD is supported in part by JSA, LLC under DOE contract No. DE-AC05-06OR-23177 and by the Jeffress Memorial Trust, J-968. WD and SM are supported by DOE OJI Award DE-SC000-1784 and DOE grant DE-FG02-04ER41302. CJDL is supported by NSC grant number 99-2112-M-009-004-MY3. We acknowledge the hospitality of Academia Sinica Taipei and NCTS Taiwan. This research made use of computational resources provided by NERSC and the NSF Teragrid.

References

[1] M. B. Wise, Phys. Rev. D **45**, 2188 (1992); G. Burdman, J. F. Donoghue, Phys. Lett. B **280**, 287 (1992); T. M. Yan *et al.*, Phys. Rev. D **46**, 1148 (1992); P. L. Cho, Nucl. Phys. B **396**, 183 (1993).

[2] A. S. Kronfeld, S. M. Ryan, Phys. Lett. B **543**, 59 (2002).

[3] T. Mannel, S. Recksiegel, J. Phys. G **24**, 979 (1998).

[4] G. M. de Divitiis *et al.* (UKQCD Collaboration), JHEP **10**, 010 (1998); A. Abada *et al.*, JHEP **0402**, 016 (2004); S. Negishi, H. Matsufuru, T. Onogi, Prog. Theor. Phys. **117**, 275 (2007); H. Ohki, H. Matsufuru, T. Onogi, Phys. Rev. D **77**, 094509 (2008); D. Bećirević *et al.*, Phys. Lett. B **679**, 231 (2009); J. Bulava, M. A. Donnellan, R. Sommer, PoS **LATTICE2010**, 303 (2010).

[5] W. Detmold, C.-J. D. Lin, S. Meinel, arXiv:1109.2480.

[6] W. Detmold, C.-J. D. Lin, S. Meinel, JLAB-THY-11-1459.

[7] W. Detmold, C.-J. D. Lin, S. Meinel, arXiv:1108.5594.

[8] D. B. Kaplan, Phys. Lett. B **288**, 342 (1992); Y. Shamir, Nucl. Phys. B **406**, 90 (1993); V. Furman, Y. Shamir, Nucl. Phys. B **439**, 54 (1995).

[9] E. Eichten, B. R. Hill, Phys. Lett. B **240**, 193 (1990).

[10] M. Della Morte *et al.* (ALPHA Collaboration), Phys. Lett. B **581**, 93 (2004).

[11] Y. Aoki *et al.* (RBC/UKQCD Collaboration), Phys. Rev. D **83**, 074508 (2011).